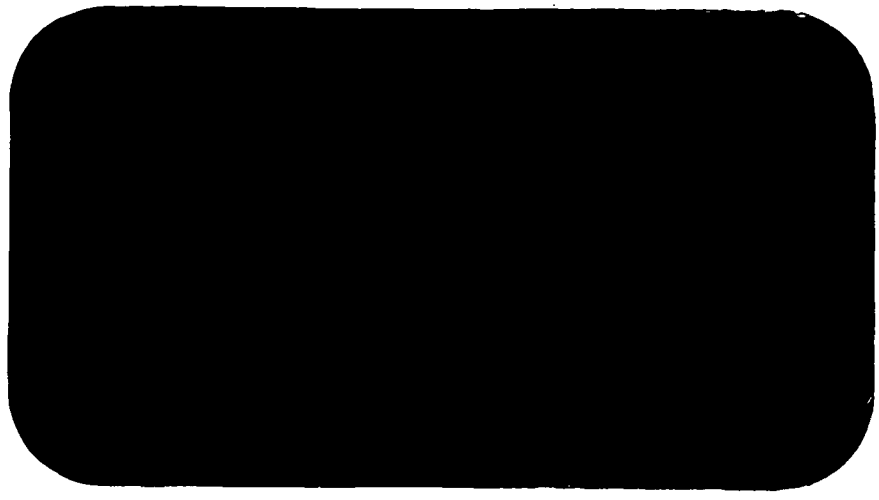

Rockwell International

(NASA-CR-178873) NON-INTRUSIVE SPEED SENSOR (Rockwell International Corp.) 47 p
CSCL 14B
N86-30125
Unclas
G3/35 43548

NON-INTRUSIVE SPEED SENSOR

NAS8-34658

FINAL REPORT

PHASE II

RI/RD 85-283

APRIL, 1986

PREPARED FOR:

NASA-MARSHALL SPACE FLIGHT CENTER

HUNTSVILLE, ALABAMA 35812

PREPARED BY

L. WYETT

MEMBER OF TECHNICAL STAFF

ADVANCED INSTRUMENTATION

APPROVED BY

S. BARKHOUDARIAN

PROJECT ENGINEER

ADVANCED INSTRUMENTATION

W. PALMQUIST

PROJECT MANAGER

ADVANCED BOOSTER PROPULSION

ABSTRACT

In Phase I of the Non-Intrusive Speed Sensor program, a computerized literature search was performed to identify candidate technologies for remote, non-intrusive speed sensing applications in Space Shuttle Main Engine (SSME) turbopumps. The three most promising technologies were subjected to experimental evaluation to quantify their performance characteristics under the harsh environmental requirements within the turbopumps. Although the infrared and microwave approaches demonstrated excellent cavitation immunity in laboratory tests, the variable-source magnetic speed sensor emerged as the most viable approach. Preliminary design of this speed sensor encountered no technical obstacles and resulted in viable and feasible speed nut, sensor housing, and sensor coil designs.

Phase II of this program developed the variable-source magnetic speed sensor through the detailed design task and guided the design into breadboard fabrication. The speed sensor and its integral speed nut were evaluated at both unit and system level testing. The final room-temperature and cryogenic spin testing of the hardware demonstrated that the sensor was capable of generating sufficient output signal to enable remote speed sensing from 1500 to 40000 rpm over a speed nut/sensor separation of 3.5 inches.

INTRODUCTION

Reusable rocket engines such as the Space Shuttle Main Engines (SSME) and the Orbital Transfer Vehicles (OTV) have throttling capabilities that require real-time, closed-loop control systems of engine propellant flows, combustion temperatures and pressures, and turbopump rotary speeds. In the case of the SSME, there are four turbopumps that require real-time measurement and red-line control of their rotary speeds. Variable-reluctance magnetic speed sensors were designed, fabricated, and tested for all four turbopumps, resulting in the successful implementation and operation of three of these speed sensors during each of the 25 Shuttle flights. The fourth speed sensor, Figure 1, designed for the High Pressure Oxidizer Turbopump (HPOTP), shown in Figure 2, was removed from all flights and ground tests due to structural weaknesses of its 3.5-inch long intrusive probe tip, which had to withstand 200 ft/sec flow velocities and 34.5 g_{rms} vibration in a liquid-oxygen environment where loose-part collisions can have catastrophic consequences. The probe tip, shown in Figure 3, could not have been shortened because the signal amplitude would have been reduced to less than 20 microvolts at 500 rpm for a 3.5-inch separation between the speed nut and the pickup coil. This is an impractical signal level for SSME applications.

To overcome this problem, a technology program was initiated by MSFC resulting in a contract award to Rocketdyne. The timeline of this program is shown in Table 1. This program consisted of identification, analysis, experimental evaluation of non-intrusive speed measurement techniques, a tradeoff study, and preliminary design of a selected non-intrusive speed sensor capable of measuring the speed of any SSME turbopump over its normal operating range with $\pm$25 rpm accuracy.

HPOTP SPEED SENSOR

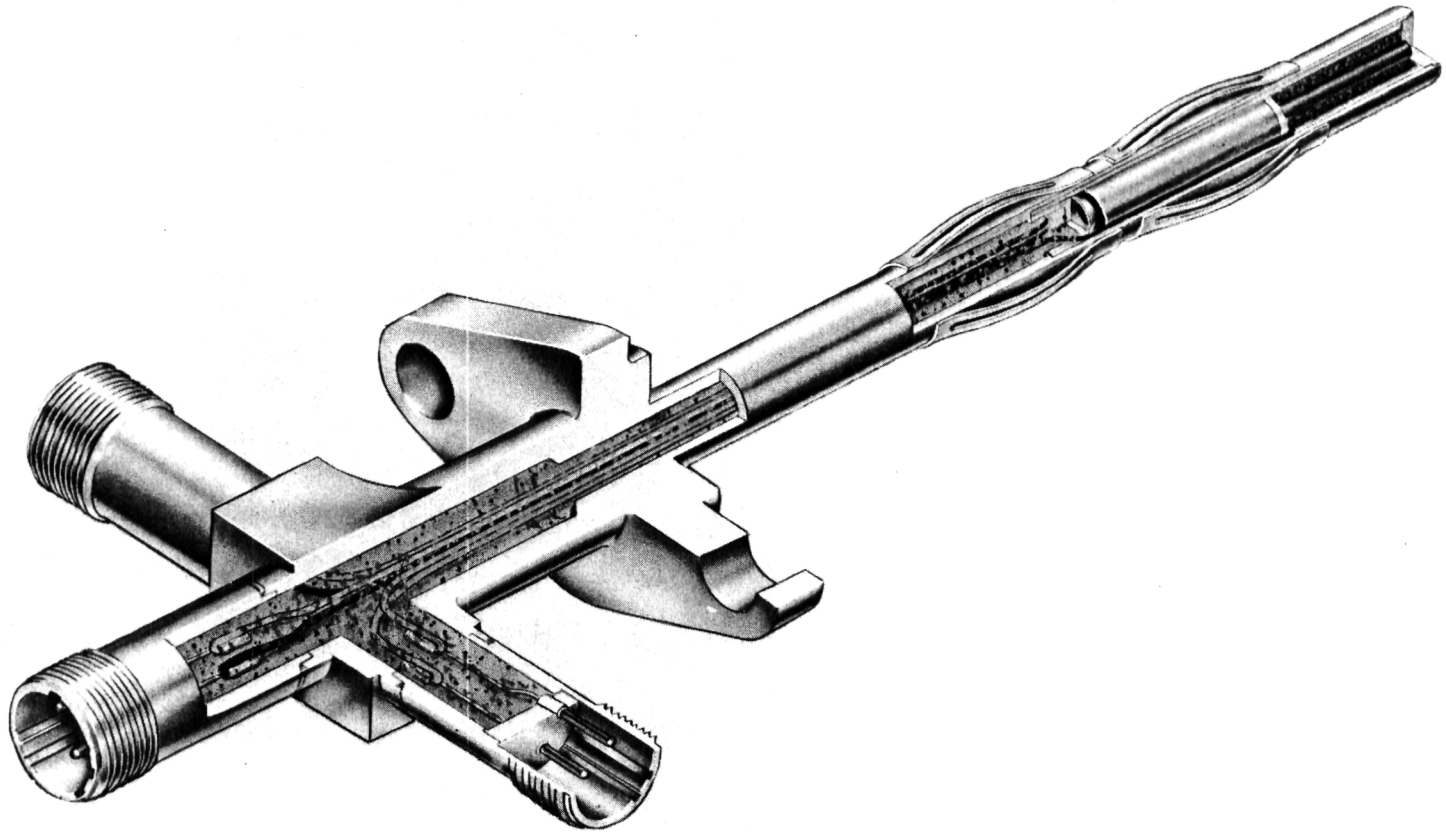

LC30D-261A

Rockwell International
Rocketdyne Division

Figure 1

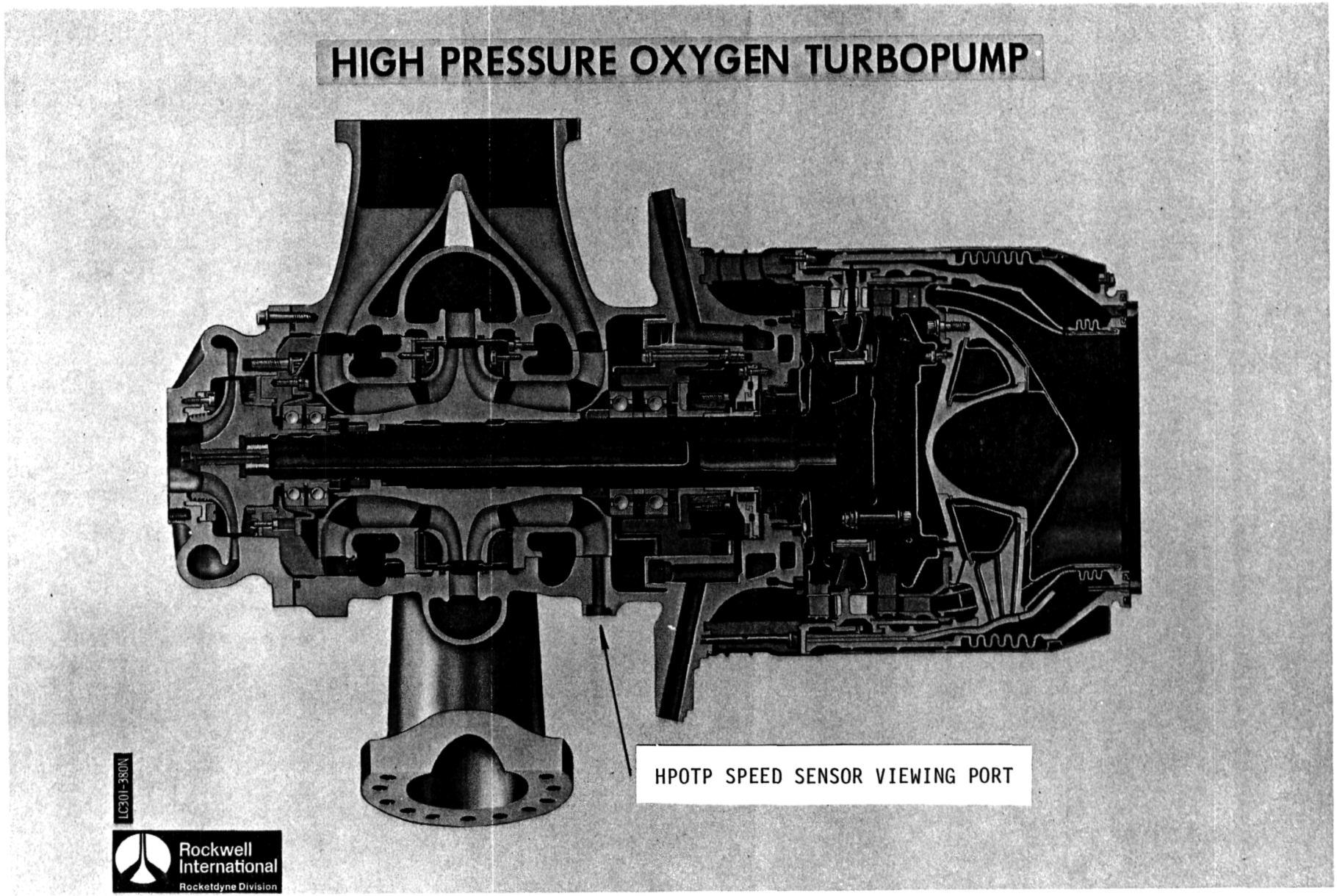

Figure 2

EXISTING SSME SPEED SENSOR

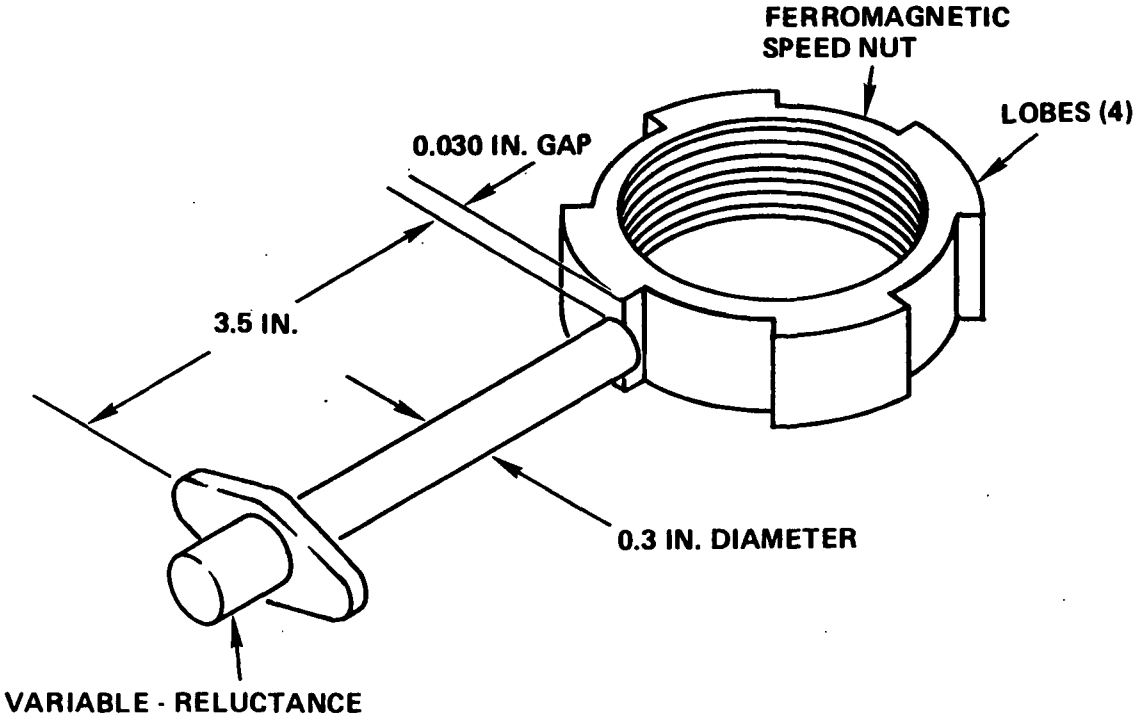

487-695

Rockwell International
Rocketdyne Division

Figure 3

TABLE 1

PROGRAM PLAN

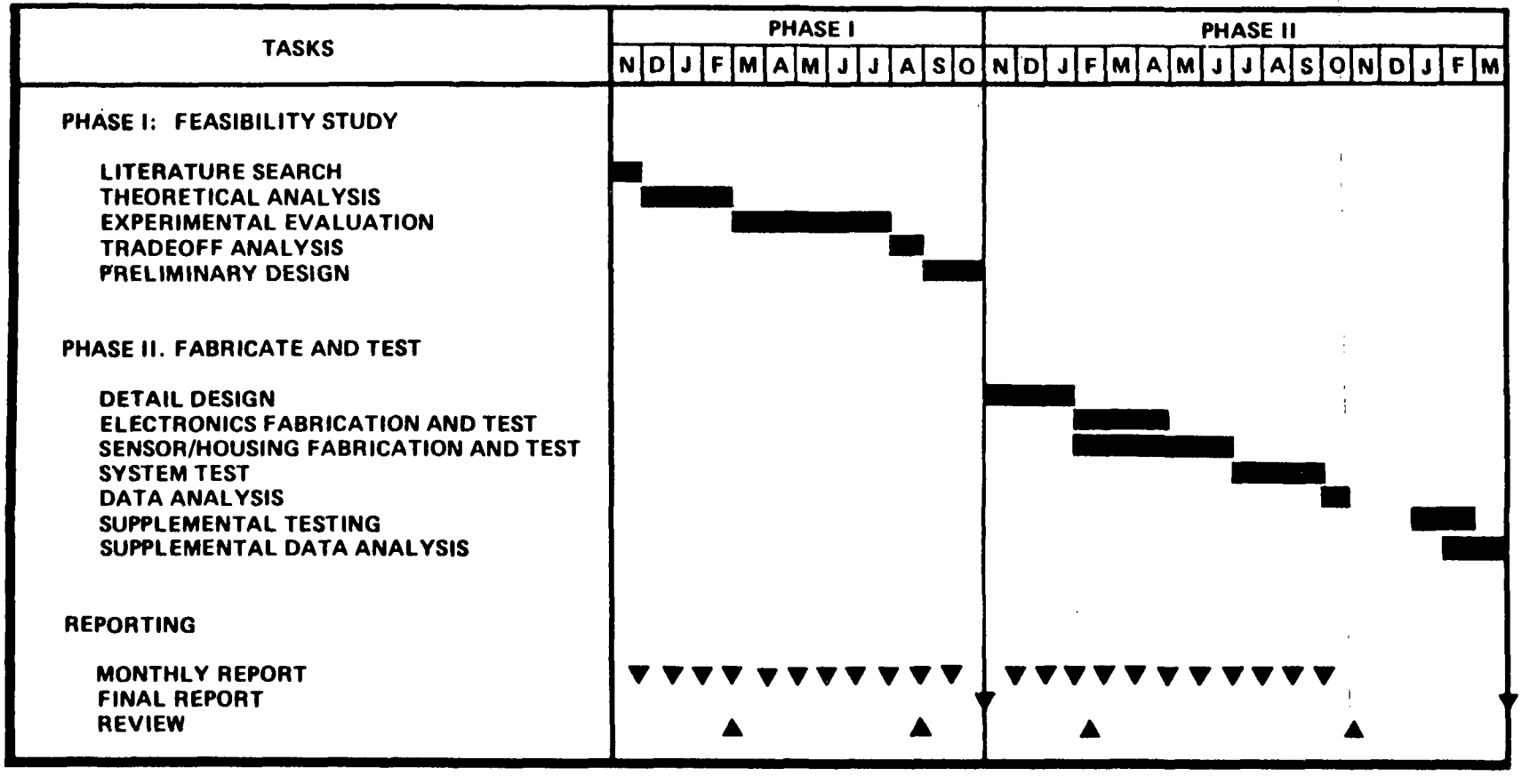

485-988C

Rockwell International
Rocketdyne Division

PROGRAM SUMMARY

PHASE I

Phase I of the non-intrusive speed sensor program was completed within budget and ahead of schedule: the 12 months of tasks were completed in only 10 months. During the period, the following accomplishments were achieved:

Task I - Literature Search

Computerized literature searches were performed to identify published articles related to non-intrusive measurement techniques. These searches yielded 550 citations from which 42 articles were obtained for review. Six new technologies were obtained from the search and supplemented the 8 technologies already known to us, resulting in 14 identified non-intrusive/remote speed sensing technologies.

Task II - Technology Evaluation

All 14 technologies were subjected to thorough theoretical evaluation to quantify their performance characteristics. Based upon the calculations of anticipated signal levels and environmental compatibilities, three promising technologies emerged from the analysis and were recommended for experimental evaluation: the variable-source magnetic approach, the infrared approach, and the microwave approach (Table 2).

TABLE 2

CANDIDATE REMOTE/NON-INTRUSIVE SPEED SENSING TECHNOLOGIES

TECHNOLOGY	ANALYSIS APPROACH	CRITICAL PARAMETER
VARIABLE-SOURCE MAGNETIC HALL-EFFECT WIEGAND-EFFECT	MAGNETICS	LOW-RPM SIGNAL AMPLITUDE
INFRARED MICROWAVE AMPLITUDE MODULATION ELECTROMAGNETIC DOPPLER SHIFT	ELECTROMAGNETIC WAVE THEORY	CAVITATION/BUBBLE ATTENUATION
ACCELEROMETER FIBEROPTIC PROXIMETER PRESSURE PULSATION ACOUSTIC	FAST FOURIER TRANSFORMS	INTERMITTENCE, LOW-RPM SIGNAL AMPLITUDE: UNRELIABLE
CAPACITANCE EDDY CURRENT ELECTROMAGNETOACOUSTIC	LUMPED ELECTRICAL CIRCUIT ELEMENTS	AMPLITUDE SENSITIVITY 1:10,000
ISOTOPE	ISOTOPES	HIGH-RPM ACCURACY

Task III - Experimental Evaluation

The variable-source magnetic speed sensor was tested in the laboratory to determine the output signal amplitude at low speeds and large coil/magnet separations. Strong output signals were achieved by inserting rare-earth permanent magnets in the speed nut, by increasing the coil area and number of turns, and by introducing a high permeability core material into the coil: a 9.5 mV signal was achieved at 600 rpm and a 3.5-inch separation using samarium cobalt magnets and a 1000-turn 7/8x7/8 inch coil with a HY-MU-80 core. Additional tests were performed to quantity the shielding effect of turbine blades and turbopump housing materials on the sensitivity of this new sensor. It was found that intervening Inconel 718 material had no noticeable attenuation effects on the sensor output signal up to 6000 rpm, which demonstrated the feasibility of mounting the variable-source magnetic speed sensor completely externally on the turbopump housing.

The infrared technology was tested for its immunity to attenuation effects from intervening cavitation (bubbles) in the liquid oxygen medium. The infrared cavitation experimentation determined the relative transmittance of visible and infrared light through a liquid medium with controllable levels of induced cavitation. It was found that, for bubbles of 0.01-0.5 centimeter radii, the liquid medium demonstrated very acceptable transmission characteristics for both visible and near-infrared light resulting in only 50% loss in transmission at the 6% cavitation level, in accordance with the Mie scattering calculations for these conditions. Confirmation of the feasibility of the visible/infrared approach would require an operating HPOTP under cryogenic and high pressure conditions.

The microwave technology must satisfy the same cavitation immunity requirements as the infrared technology. Our experiments indicated that nitrogen bubbles in liquid nonane only serve to change the cavity resonance modes of the waveguide, and have little or no signal attenuation effects on microwave energy transmittance. This technology must also prove itself on an operating HPOTP to verify its feasibility under cryogenic, high pressure conditions.

In short, all three of the technologies recommended on the basis of theoretical analysis came through the experimental evaluation showing promise as viable speed sensing technologies.

Task IV - Tradeoff Analysis

Given that further experimental evaluation would be required to demonstrate the viability of the infrared and microwave technologies in the actual HPOTP operating environment, the variable-source magnetic speed sensor immediately presented itself as the candidate for preliminary design (Table 3). This magnetic approach requires no controller modification and uses space-proven hardware, in addition to its inherent cavitation immunity. The possibility of mounting such a sensor completely outside the HPOTP makes the variable-source magnetic speed sensor a very attractive technology worthy of further development.

TABLE 3

TASK IV – TRADEOFF STUDY

FEATURE	MAGNETIC	INFRARED	MICROWAVE
CONTROLLER MODIFICATION	NONE	SLIGHT	SLIGHT
SPACE-PROVEN HARDWARE	YES	NONE	PARTIAL
CONSTANT AMPLITUDE	NO	YES	YES
CAVITATION IMMUNITY	EXCELLENT	LIMITED	GOOD

Task V - Preliminary Design

The preliminary design of the variable-source magnetic speed sensor was performed for the speed nut, probe, and electrical components. The proposed speed nut, which contains four magnets equally spaced around its periphery, was subjected to a preliminary stress analysis which indicated that magnets of sufficient size can be accommodated into the speed nut without adverse stress effects.

The preliminary probe design utilized a modified sensor housing from the existing HPOTP speed sensor and removes the sensing elements to outside the liquid oxygen environment. This sensor used the same mounting holes as the present speed sensor, thus requiring no modification of the HPOTP housing.

The preliminary design of the electrical components resulted in a design which meets the controller requirements of 75mV minimum signal and 3000 Hz frequency response while increasing the probe gap from 0.030 to 3.5 inches.

In summary, the preliminary design task indicated no obstacles in implementing the variable-source magnetic speed sensor approach.

RECOMMENDATION

It was recommended that Phase II be initiated to fully develop the variable-source magnetic speed sensor for eventual incorporation into the existing SSME HPOTP.

PROGRAM OBJECTIVE

PHASE II

The objective of Phase II of the Non-Intrusive Speed Sensor program was to develop and fabricate a working breadboard of a non-intrusive speed sensor which will be potentially applicable to an SSME High Pressure Oxidizer Turbopump. The theoretical analyses and breadboard evaluation of many non-intrusive rotational speed sensing techniques were performed in Phase I of this program, resulting in the recommendation of the variable-source magnetic speed sensor for further development during Phase II. The sensor has undergone detailed design, fabrication, unit testing, system level testing, and additional cryogenic spin testing at MSFC request before delivery to the Marshall Space Flight Center at the end of this 15-month program.

DETAILED DESIGN - SPEED SENSOR

The feasibility of the variable-source magnetic speed sensor as a remote measurement technique was thoroughly demonstrated in Phase I of this program. It was the purpose of the Detailed Design Task of Phase II to develop this sensor into a final design package suitable for fabrication. The initial thrust of these efforts was to investigate methods of increasing the speed sensor output signal voltage to meet the 75mV signal level required by the SSME controller for the minimum required shaft speed of 1500 rpm. Based upon the preliminary design work performed in Phase I of this program, there were several approaches to maximizing the sensor output voltage:

- Investigate alternate orientations and configurations of the magnets.
- Investigate inherently stronger magnetic materials.
- Increase the allowable volume of magnets in the speed nut.
- Select high permeability sensor core materials.
- Shape the core to concentrate the magnetic field at the sensor.
- Increase the cross-sectional area of the sensor coil.
- Increase the number of windings in the sensor coil.

These approaches will now be discussed at length to show how each was applied to the Non-Intrusive Speed Sensor breadboard design.

Magnetic Orientations/Configurations: The effects of various magnetic arrangements were quantified with a series of experimental layouts as shown in Figure 4. A 2.625-inch diameter Inconel wheel simulating a speed nut was fixed onto a motorized shaft, and a selection of 0.25-inch diameter by 0.10-inch thick samarium cobalt magnets were secured to the outside edge of the wheel. A 1000-turn sensor coil was normally located 3.5-inches from the magnets and looked radially toward the rotating shaft. The previous Phase I experiments were repeated with these standard magnets to establish an accurate baseline for determining the sensor output voltages and the improvements obtained with new sizes, shapes, compositions, orientations, and configurations of magnets.

It is possible to place a magnet of the outer edge of the wheel in any of three orientations:

(1) With its axis of magnetization pointed radially outward from the shaft.
(2) With the axis pointed tangentially to the outer edge, in the plane of the wheel.
(3) With the axis aligned with the axis of rotation of the wheel.

These radial, tangential, and axial orientations were investigated and combined to yield over 30 combinations of magnets for experimentation. The two most promising configurations, along with the preliminary design configuration for comparison, are shown in Figure 5. Figure 6 shows the relative merits of these two approaches. The Radial #2 configuration (NSNS)

FLUX ENHANCEMENT CONFIGURATIONS

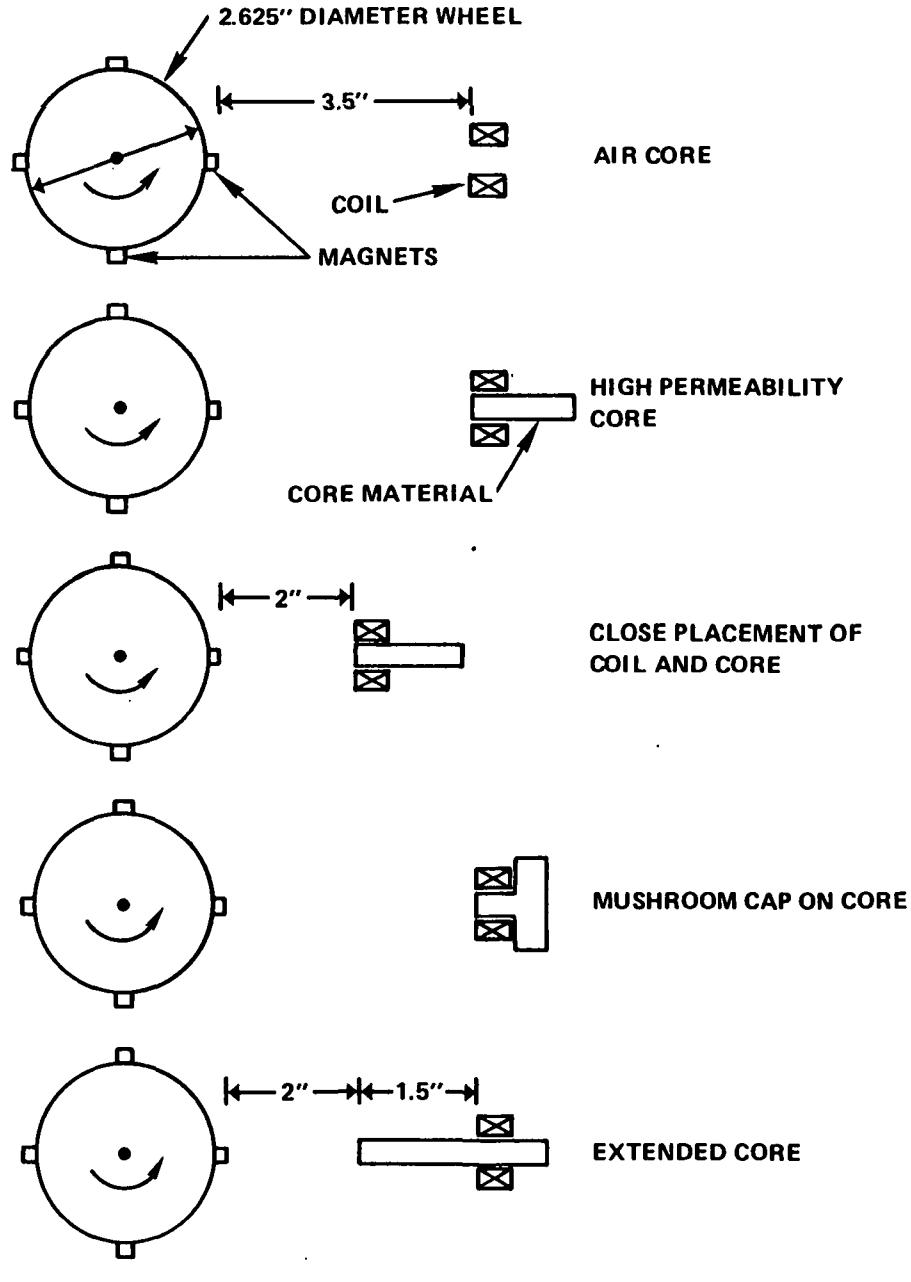

490-769

Rockwell International
Rocketdyne Division

Figure 4

SIGNAL ENHANCEMENT EXPERIMENTATION

	RADIAL NO. 1	RADIAL NO. 2	TANGENTIAL
SEPARATION d	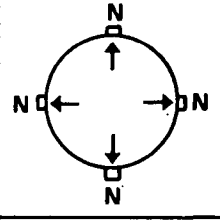	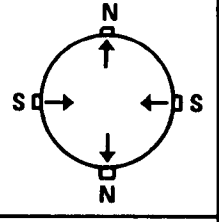	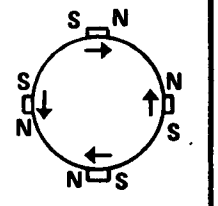
AIR CORE			
3.5"	0.4 mV PEAK	1 mV PEAK	1.2 mV PEAK
2"	3	4	6
HY-MU-80 CORE			
3.5"	1	2.6	2.9
2"	9	11	15

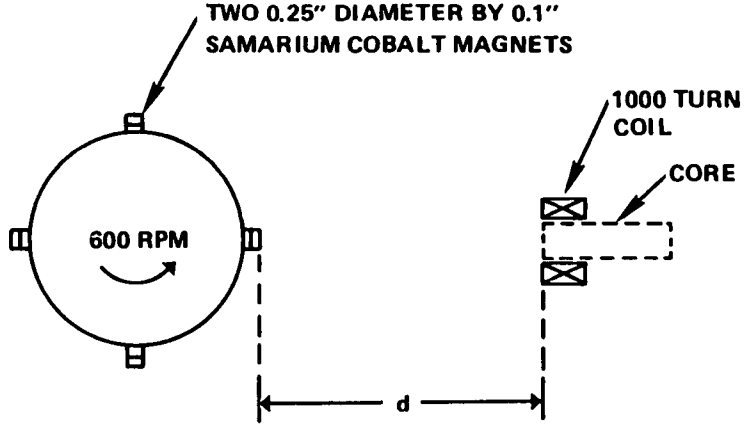

490-775

Rockwell International
Rocketdyne Division

Figure 5

THEORETICAL SIGNAL STRENGTHS FOR RADIAL AND TANGENTIAL MAGNETIZATION

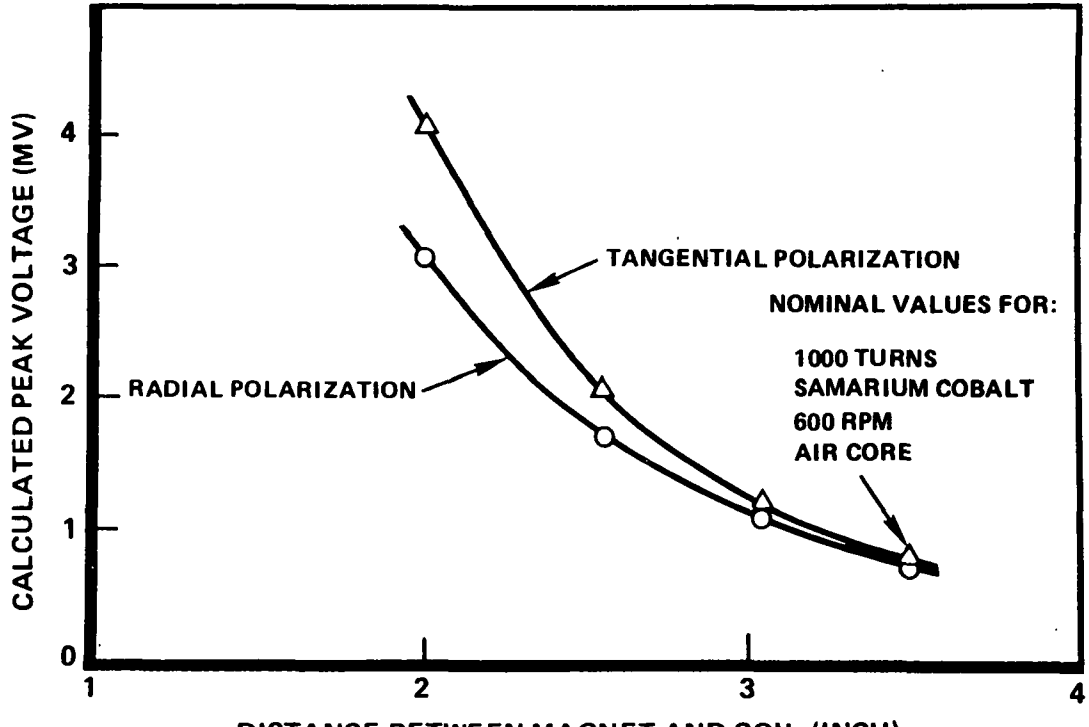

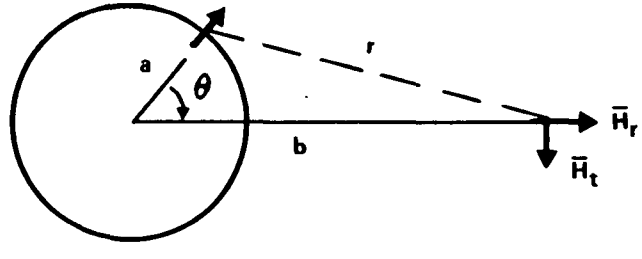

$r^2 = a^2 + b^2 - 2ab\cos\theta$

$$V_r = k_2(2ab\sin\theta)/r^5 \left\{ 20ab/r^2 \left[(\cos\theta - a/b)(b/a - \cos\theta) \right] + 2(\cos\theta - b/a - a/b) \right\}$$

$$V_t = k_2 \frac{2}{r^7} \left\{ r^2\cos\theta\,(3a^2 - 3b^2 - r^2) + 3ab\sin^2\theta\,(r^2 + 5b^2 - 5a^2) \right\}$$

490-767

Rockwell International
Rocketdyne Division

Figure 6

was selected for its relative ease of implementation into the speed nut. The Tangential approach was rejected due to difficulties in achieving Stress Dynamics approval and due to uncertainties in guaranteeing the precise orientation of the imbedded magnets.

Magnetic Materials: Samarium cobalt magnets were chosen for the baseline studies of sensor output voltages due to their greater magnetic field strength over that of Alnico, ceramic, or ferrite magnets. During the course of these experiments, a new magnetic material of iron-neodymium-boron composition was brought into production by Crucible, Inc. under the trade name of Crumax 35. This material was reported to exhibit substantially greater magnetic field strength that of even samarium cobalt magnets, and preliminary trials with this material suggested 30% greater sensor output over that of the standard magnets. Crumax 35 was thus selected for use in the speed nut.

Magnet Volume: Some of the configuration studies involved stacking multiple standard magnets and observing the effect on the output signal of the sensor coil. It was found that the induced output voltage was directly proportional to the number of magnets present at each location. Additionally, it was found that for a given number of magnets, the stacked magnetic configuration and a side-by-side configuration induced the same output voltage in these tests, indicating that it is the volume rather than the shape of the magnetic material which determines the output voltage. Thus, the maximum attainable magnet volume in the speed nut was sought by Stress Dynamics while the minimum required volume was reduced to 0.01 cubic inch per magnet by the other signal enhancement techniques discussed here.

High Permeability Core: The existence of a metallic core down the axis of the sensor coil was shown in Phase I studies to increase the output voltage by a least a factor of two over the air-core trials. The choice of a high permeability core material could increase the signal by factors of 5-10 over the air-core case. To this end, HY-MU-80 was chosen as the core material based upon its high permeability and its thermal expansion characteristics.

Core Shape: Two approaches to core shaping were found to have promising effects on the output signal level: extending the core towards the speed nut as much as possible without violating the non-intrusiveness of the design, and adding a mushroom cap to the distal end of the core to help concentrate the magnetic field through the sensor coil. Figure 7 shows the effectiveness of these approaches. As can be seen in the final design drawing (Figure 8), both approaches were utilized. The addition of the mushroom cap alone increased the signal level by more than 30%.

Coil Cross-Sectional Area: The physical limitation to increasing the coil area was the mounting bolt spacing for the sensor. This spacing was to be the same as that of the old speed sensor to prevent additional changes to the HPOTP. As shown in Figure 8, the outer diameter of the sensor housing could be no more than 1.00 inch to ensure proper bolt clearances. A thorough Stress Dynamics analysis of a sensor housing composed of Inconel 718 was performed for cantilever, vibration, and pressure-related stresses anticipated on the production version of such a sensor. A 0.040-inch wall thickness was analyzed for 333g transient shock loads and demonstrated factors of safety of 2.66 on

EXPERIMENTAL FLUX ENHANCEMENT OF MUSHROOMED AND EXTENDED CORES

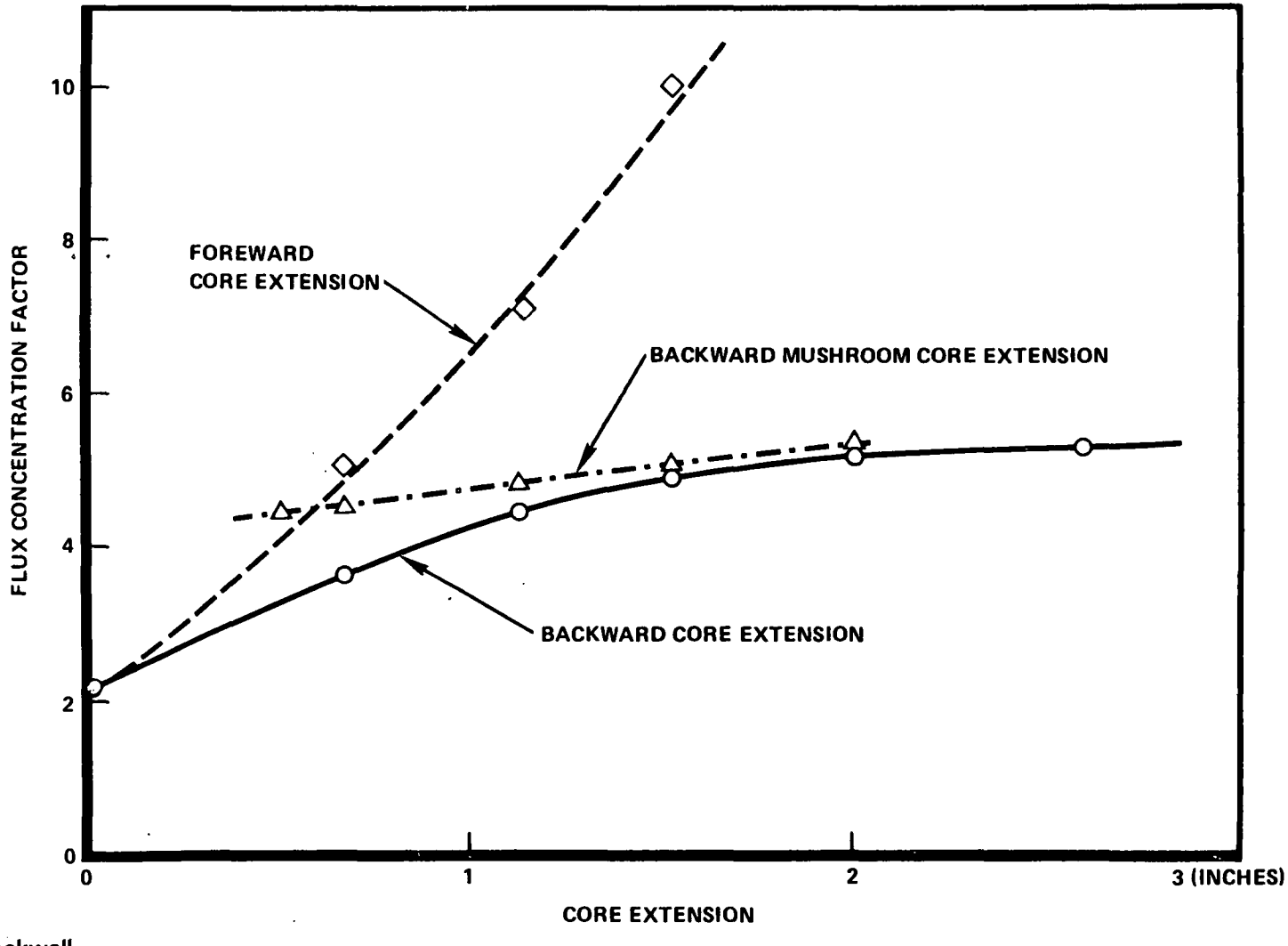

490-768

Rockwell International
Rocketdyne Division

Figure 7

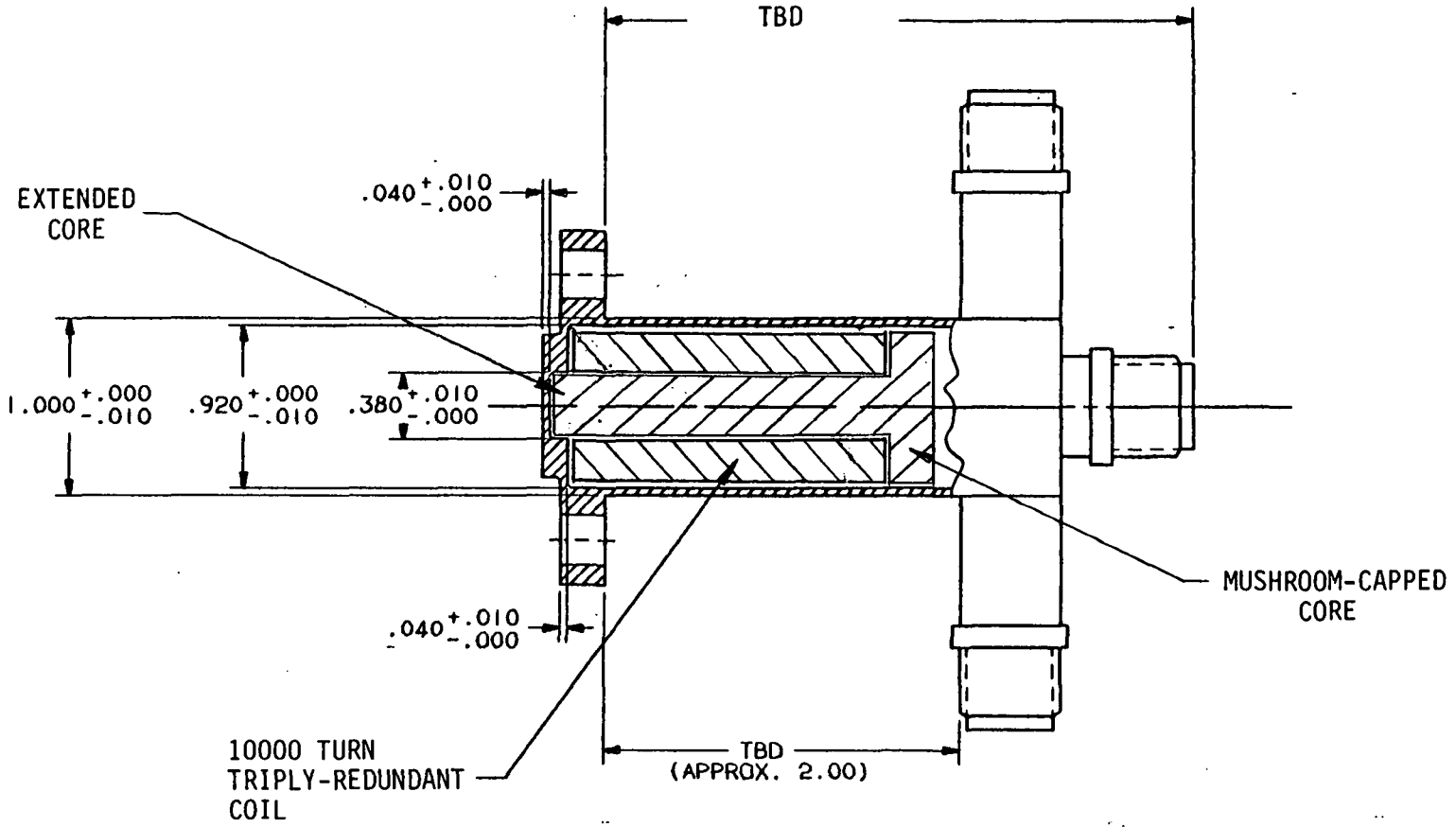

NON-INTRUSIVE SPEED SENSOR

Figure 8

yield and 3.19 on ultimate. A steady-state random vibration analysis was performed, based upon a 28g rms vibration, and this high-cycle fatigue study met life requirements by showing a factor of safety on endurance of 36.9. The proximal end cap of the sensor housing, exposed to the pump operating pressure of 1000 psi, showed factors of safety of 3.04 on yield and 3.66 on ultimate.

Coil Windings: Given the diametrical constraints on the coil, increasing the number of turns on the coil would require either increasing the length of the coil or reducing the wire gage to fit more turns into the same coil volume. #42 gage wire was determined to be the smallest diameter wire which could be wound reliably. Thanks to all the above output signal improvements, it was determined that 10,000 turns of triply-redundant wire would be sufficient to satisfy the 75mV output signal required for a sensor operating 3.5-inches from the new speed nut rotating at 1500 rpm.

DETAILED DESIGN - SPEED NUT

The key steps in finalizing the speed nut designs involved

(1) determining the composition of the speed nut,

(2) determining the number of lobes on this nut, and

(3) calculating the maximum allowable magnet volume available in the nut.

Composition: The current HPOTP speed nut is manufactured from K-Monel, an alloy which becomes ferromagnetic at cryogenic temperatures. A K-Monel speed nut with imbedded magnets would tend to trap the magnetic fields within the nut at low temperatures, thus reducing the magnetic field strength at the remote speed sensor. The solution to this problem was to fabricate the nut from Inconel 718, the same material as the HPOTP housing, which will not become ferromagnetic during cryogenic operation.

Lobes: The present speed nut has four lobes, and much experimentation and analysis has shown that the paddlewheel action of the four lobes contributes to a bearing cage delamination problem which reduces the operational lifetime of the bearing. A lobeless (constant diameter) speed nut seemed to be a reasonable solution, until it was determined that a certain amount of pumping action is required of the speed nut to maintain sufficient back-pressure for LOX coolant flow through the bearing. The SSME Phase II HPOTP uses a two-lobed speed nut, and it was determined that a new speed nut in agreement with this design philosophy would be the most applicable to future SSME implementation.

The two-lobed design, however, does not provide sufficient volume to incorporate the four magnets into the speed nut. The Hydrodynamics Department at Rocketdyne determined that a two-slot speed nut would have the same required pumping action as the two-lobed nut, and offer sufficient radial thickness to incorporate the four magnets equally spaced around the nut.

Magnet Volume: Experiments in enhancing the speed sensor's output signal level had identified both the required magnetic material (Crumax 35) and the minimum required magnet volume (0.01 cubic inch each) to generate the 75mV output signal at the 1500 rpm speed. Given the suggested speed nut material and shape, Stress Dynamics determined that magnets of 0.56 x 0.316 x 0.076 inch sizes, each with a volume of approximately 0.0123 cubic inches, were allowable in the speed nut. The magnets were first electroless copper plated, then were initially held in their machined slots with a silver-based epoxy, and then nickel-plated over to ensure LOX isolation, since LOX compatibility has not been demonstrated for this magnetic material.

With these requirements satisfied, the material properties of the final speed nut design allow a factor of safety for high cycle fatigue to be 1.7 based upon loads corresponding to the current HPOTP design at 31000 rpm. The maximum allowable speed for spin testing was determined to be 55200 rpm based upon burst speed calculations. The speed nut design is shown in Figure 9.

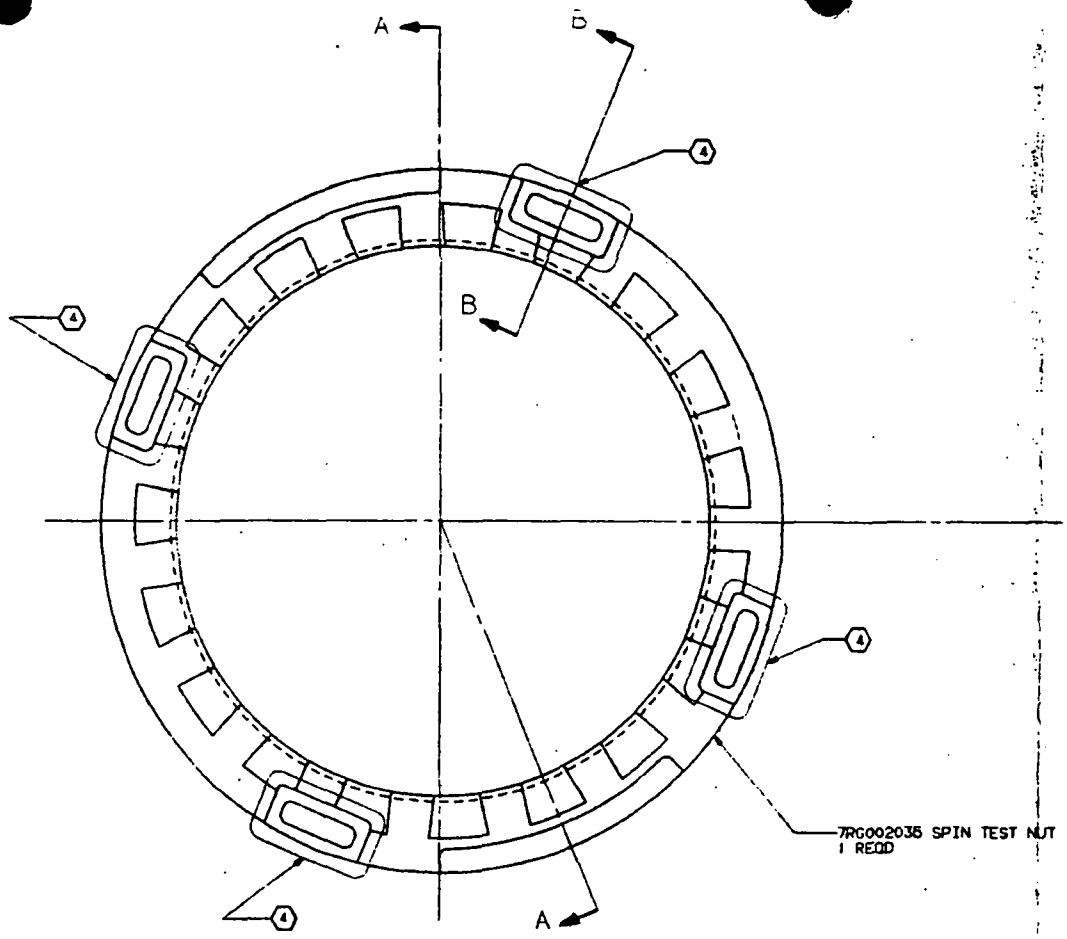

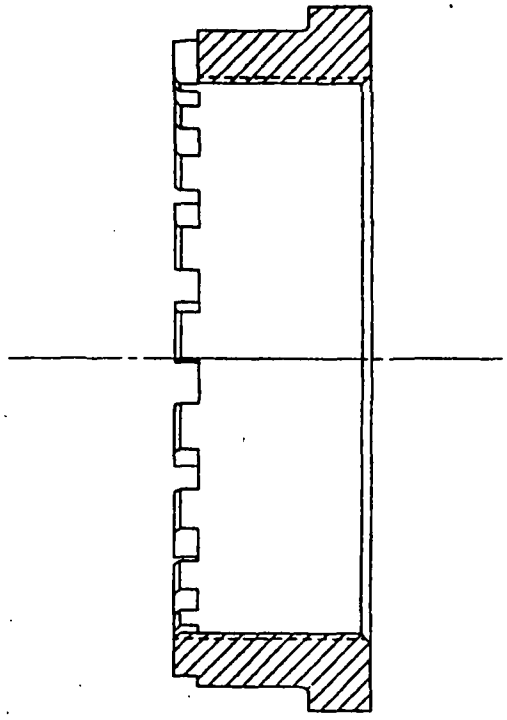

SECTION A-A

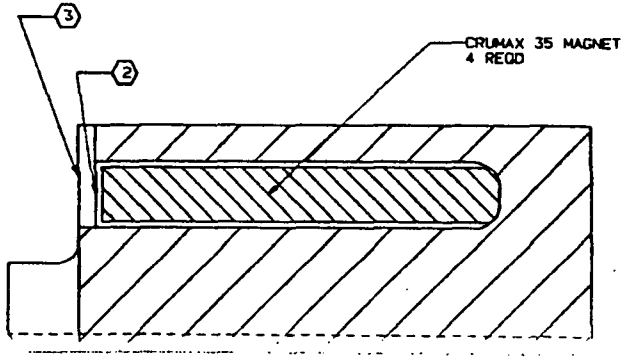

NONINTRUSIVE SPEED SENSOR

SPEED NUT

Figure 9

DETAILED DESIGN - SPIN TEST ARBOR

The completed speed nut was installed on a specially-designed aluminum spin test arbor for interfacing to an air turbine-driven shaft. The speed nut/arbor combination design had undergone moment of inertia ratio calculations by Rotordynamics to assure that this hardware was safe to spin over the full range of speeds (0-40,000 rpm). The arbor design is shown in Figure 10, and the speed nut/arbor assembly is shown in Figure 11.

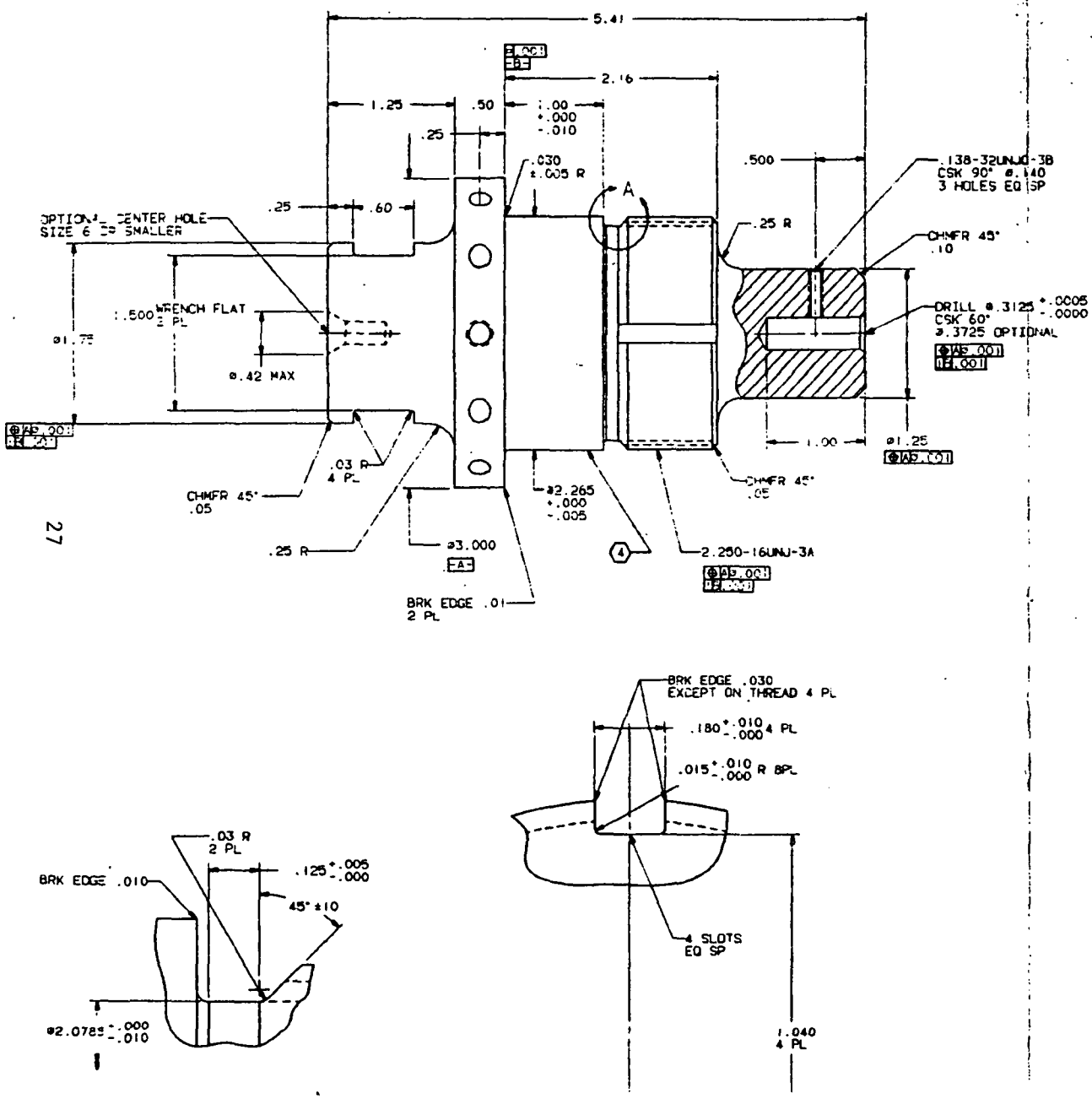

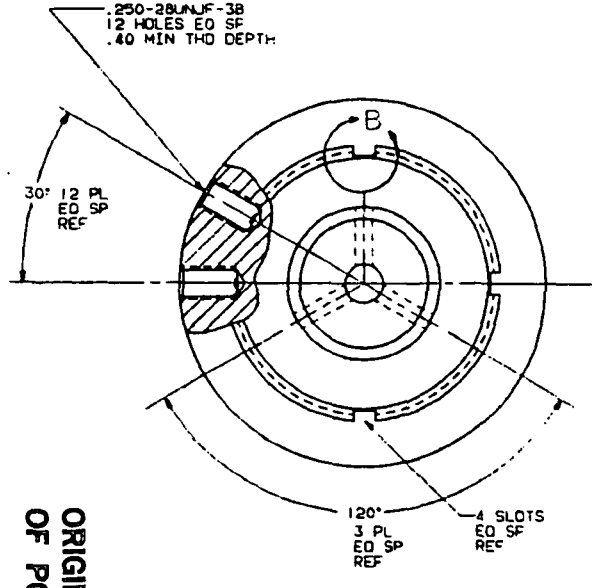

SPIN TEST ARBOR

Figure 10

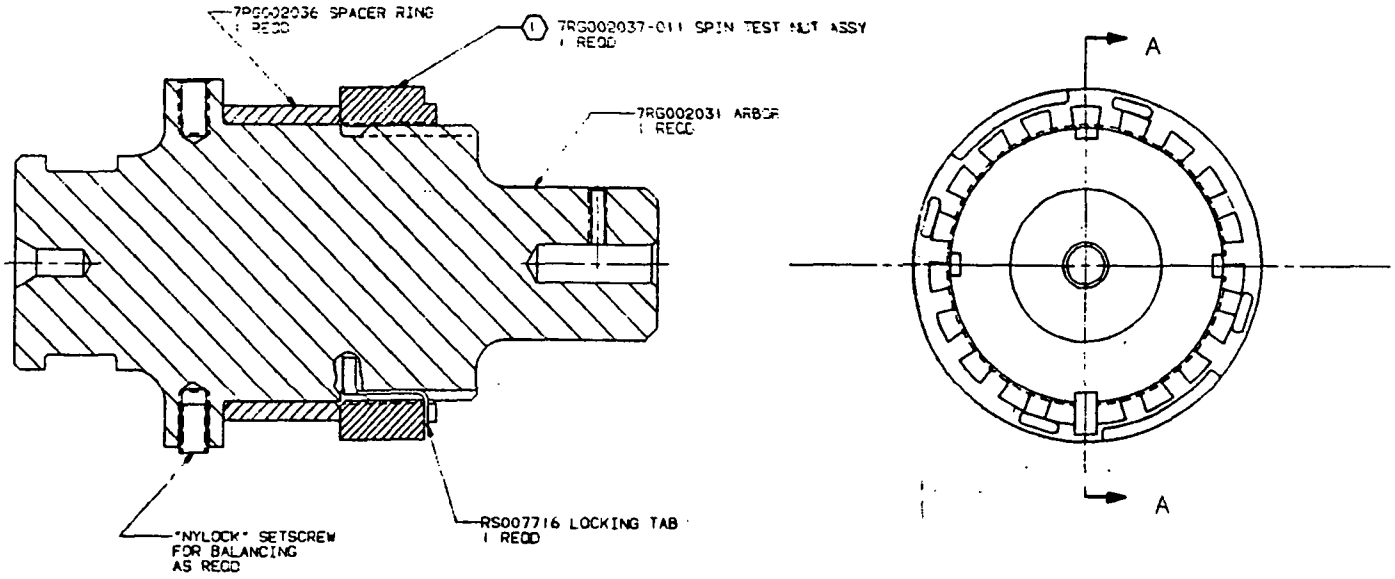

SECTION A-A

SPEED NUT / ARBOR ASSEMBLY

Figure 11

SYSTEM TESTING

Low RPM Testing

The experimental setup used to evaluate the various orientations and configurations of magnets in a simulated speed nut was utilized to establish the baseline operational characteristics of the breadboard non-intrusive speed sensor. This sensor was fabricated by Rosemount, Inc. as specified by the detailed design, with the exception that this sensor had only 9150 turns of tri-filar wire in the coil (rather than the specified 10000 turns) and only two of the three channels were operable due to wire breakages in fabrication. Both low and high rpm testing were performed with this sensor while a replacement sensor was fabricated to specifications.

Low rpm testing took the simulated speed nut and Crumax 35 magnets to 600 rpm and the sensor was evaluated at the 3.5 inch separation. With each channel loaded by a 12 Kohm resistor simulating the SSME controller input impedance, each sensor channel generated more than 55 mV of output signal. Extrapolating this value to a speed 2.5 times greater (1500 rpm), we expected that the sensor would generate more than 135 mV peak into the same controller impedance in the absence of eddy current effects.

High RPM Testing

Spin Pit Tests: Speed sensor signal characterization tests were performed over the 1500-40000 rpm range for the 3.5-inch speed nut-to-sensor separation case. These tests occurred in the Spin Pit facility at Rocketdyne, for which a pictorial and a schematic of the overall testing configuration are shown in Figures 12 and 13. The balanced speed nut/arbor assembly was rotated about a vertical axis while the speed sensor observed the changing magnetic fields from a prescribed distance. A total of five spin tests were run involving combinations of intervening Inconel 718 plates, holes in the plates, and temperature (Table 4). Both sensor output signals were shorted with 12.6 Kohm resistors to simulate the SSME controller input impedance that the sensor would experience under actual engine test conditions. The test results for the 3.5-inch separation case are presented in Figure 14.

A comparison of curves #1 and #4 in Figure 14 shows the similarity of the non-intrusive speed sensor performances through a 1-inch thick Inconel 718 barrier (representing a solid turbopump wall), and the same barrier with a 0.375-inch diameter hole along the sensor coil axis (representing a view down the existing HPOTP speed sensor access port). The removal of a relatively small volume of Inconel 718 housing material has little effect on the existence of eddy currents throughout the remaining volume of the barrier.

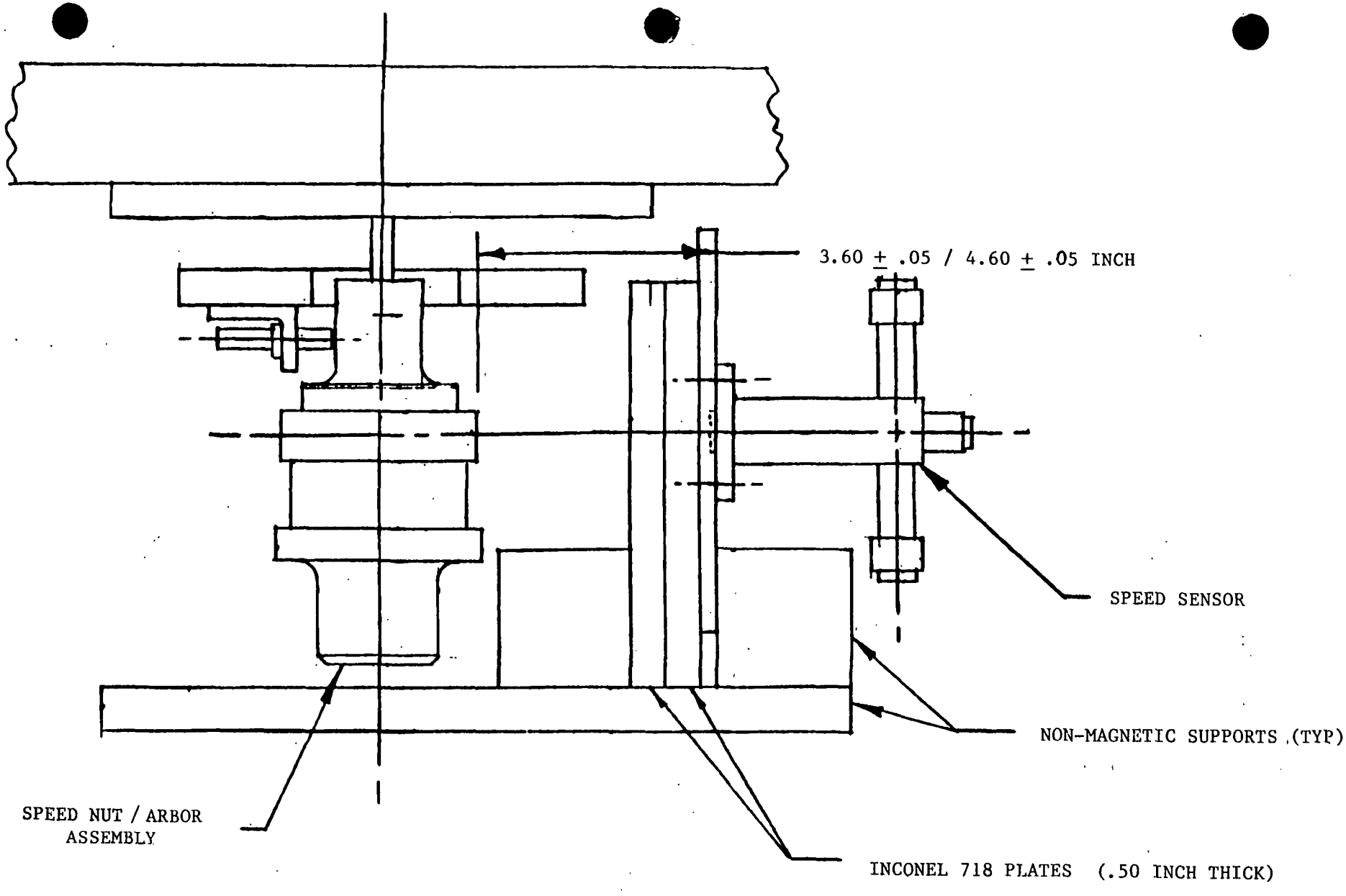

SPIN PIT INSTALLATION

FIGURE 12

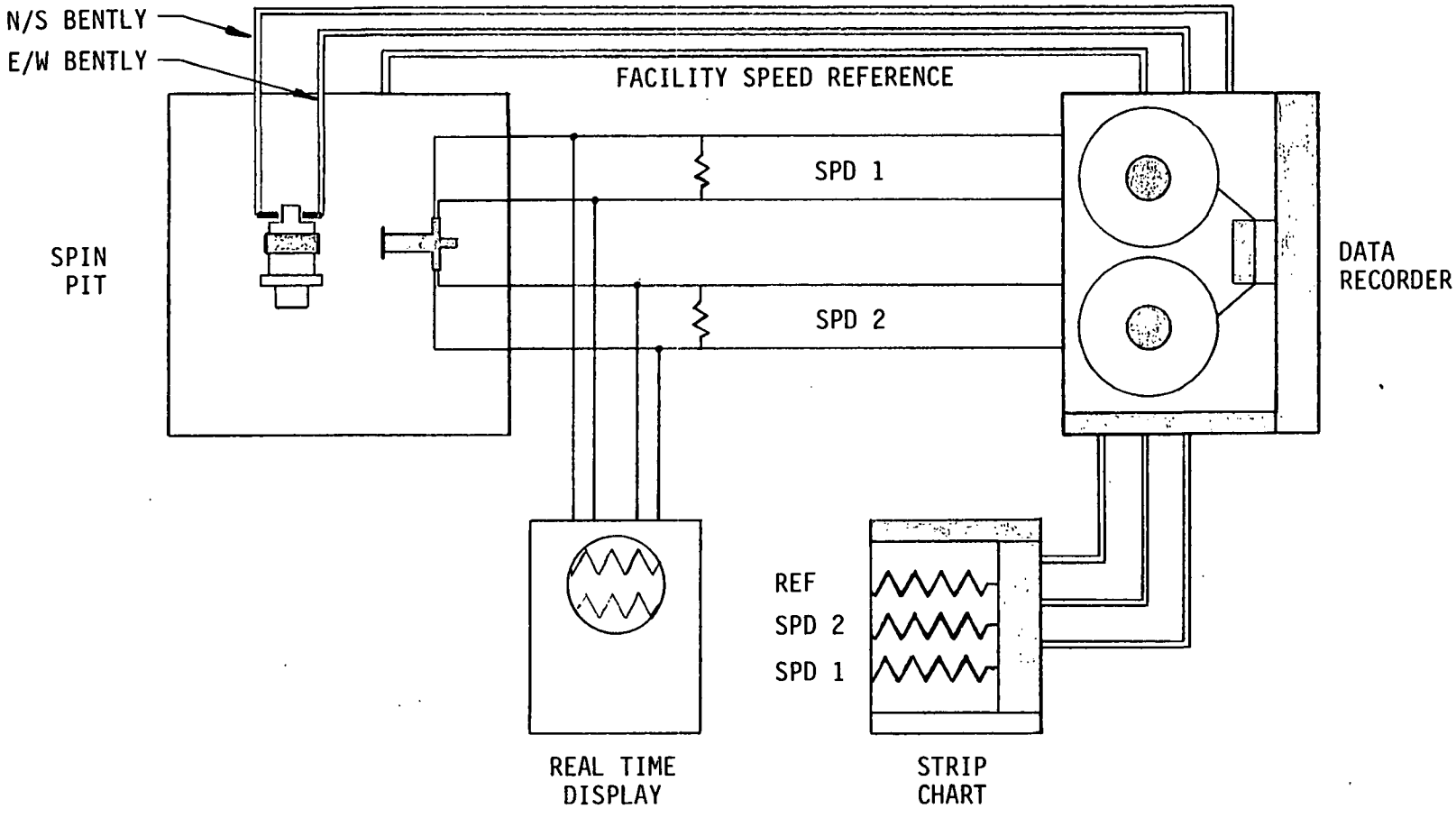

SPIN TEST SCHEMATIC
FIGURE 13

HIGH RPM SPIN TEST MATRIX

TABLE 4

TEST #	NUT-SENSOR SEPARATION	INCONEL 718 PLATES	HOLE IN PLATES	TEMPERATURE
1	3.5 INCHES	YES	NO	AMBIENT
2	4.5 INCHES	YES	NO	AMBIENT
3	3.5 INCHES	NO	--	AMBIENT
4	3.5 INCHES	YES	YES	AMBIENT
5	3.5 INCHES	YES	YES	LN_2

NON-INTRUSIVE SPEED SENSOR PERFORMANCE

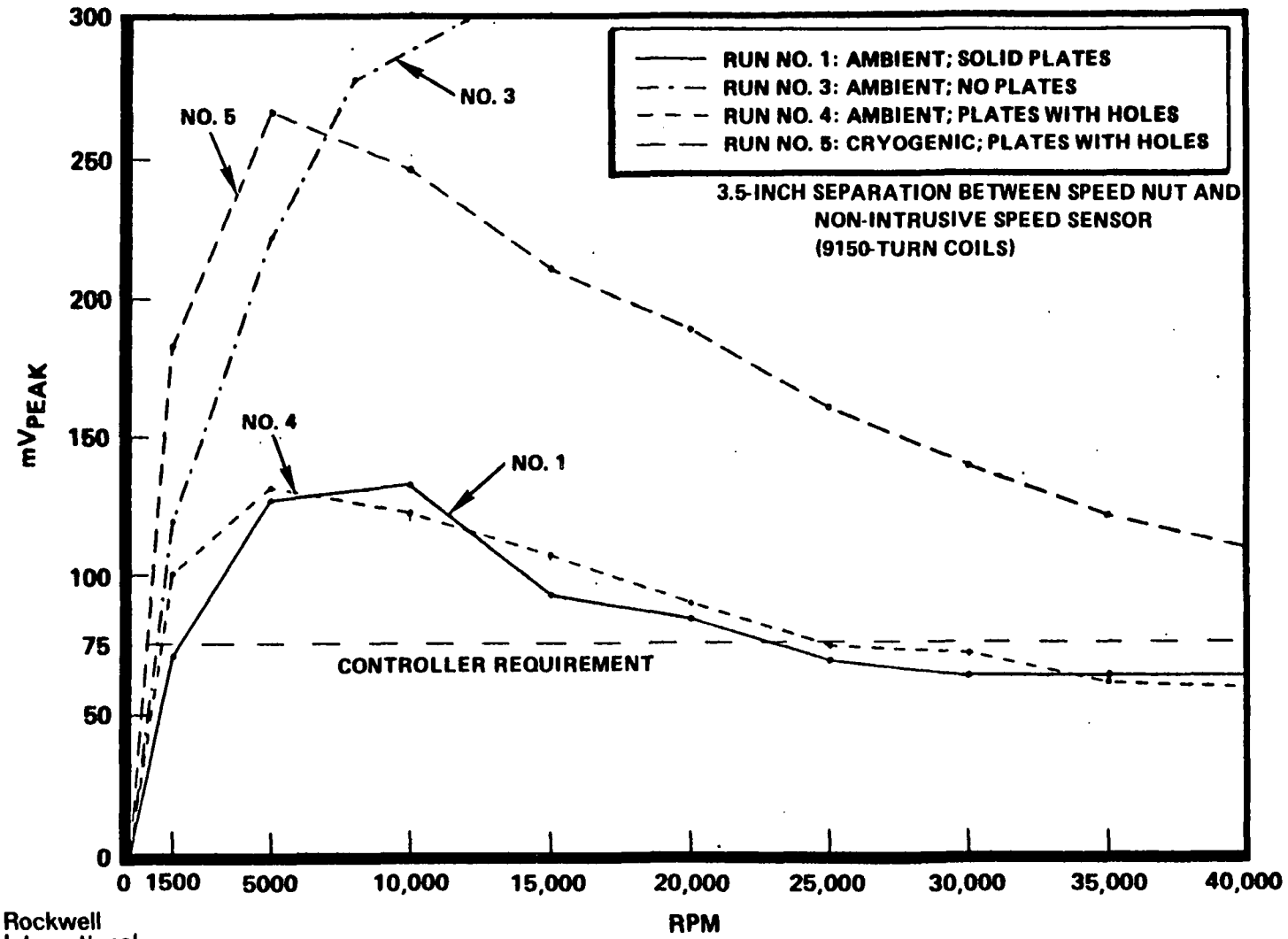

86C-9-261

Rockwell International
Rocketdyne Division

FIGURE 14

Curves #1 or #4, when compared to curve #3, show the dramatic effect of a large volume of Inconel 718 (and its inherent eddy current effects) on the speed sensor output signal level. (Test #3 was performed only to 12000 rpm due to a balancing problem with the rotating facility equipment.)

A comparison of curves #4 and #5 shows the contribution of cryogenic temperatures to speed sensor performance. The increased ratio of outputs between the curves at low frequencies is a result of sensor chilling effects. It is thought that curve #5 is artificially high due to the possible intermittent opening of one coil in the sensor during the cryogenic test run.

Laboratory Testing: The simple physical model of an open-circuited and unshielded coil exposed to a changing magnetic field predicts that the coil output voltage increases linearly with frequency. However, the experimentally determined output voltage initially rises steeply with increasing rpm, reaches a maximum in the 5000-to-15000 rpm speed range, and slowly decreases with increasing rpm beyond 15000 rpm. It is possible to reconcile these viewpoints by recognizing the existence of many distinct frequency-dependent factors which contribute to the output signal level. These factors were quantified in the second type of high rpm experiments which corroborated and explained the spin pit results. These tests were performed using a coil connected to a signal generator to serve as an oscillating magnetic dipole (replacing the rotating speed nut), which allowed sensor characterization from 50-2000 Hz (1500-60000 rpm).

Sensor Coil Termination: The impedence which the sensor observes in use can vary the output voltage level significantly. Additionally, the termination of a redundant coil also affects the output of the first coil. These impedence effects become more significant at higher frequencies, as shown in Figure 15.

Sensor Coil Temperature: The overall resistance of a coil changes significantly between ambient and cryogenic (LN_2) temperatures. Each channel of the speed sensor reduced its resistance by a factor of 8 (e.g., from 2550 ohms to 319 ohms). As this resistance change couples in with coil inductance and with mutual inductance changes, the effect becomes frequency dependent. Chilling the sensor increases its output by approximately 14% at 1500 rpm, while there is no significant signal increase at the highest frequencies. The dashed curve in Figure 15 shows this effect.

Intervening Inconel 718: The existence of Inconel 718 material between the speed sensor and the nut provides a medium for induced eddy currents to flow, causing signal reduction. The signal reduction is not noticeable at low speeds, but becomes increasingly important at higher speeds. Over the range of rpm considered here, the magnetic field frequency is sufficiently low to maintain a macroscopic skin depth, making eddy current attenuation effects dependent upon material thickness (Figure 16). The speed sensor housing, also made of Inconel 718, places intervening Inconel between the sensor coils and the speed nut. The maximum effect of this 0.040-inch thick material was found to be a 17% signal loss at 40000 rpm.

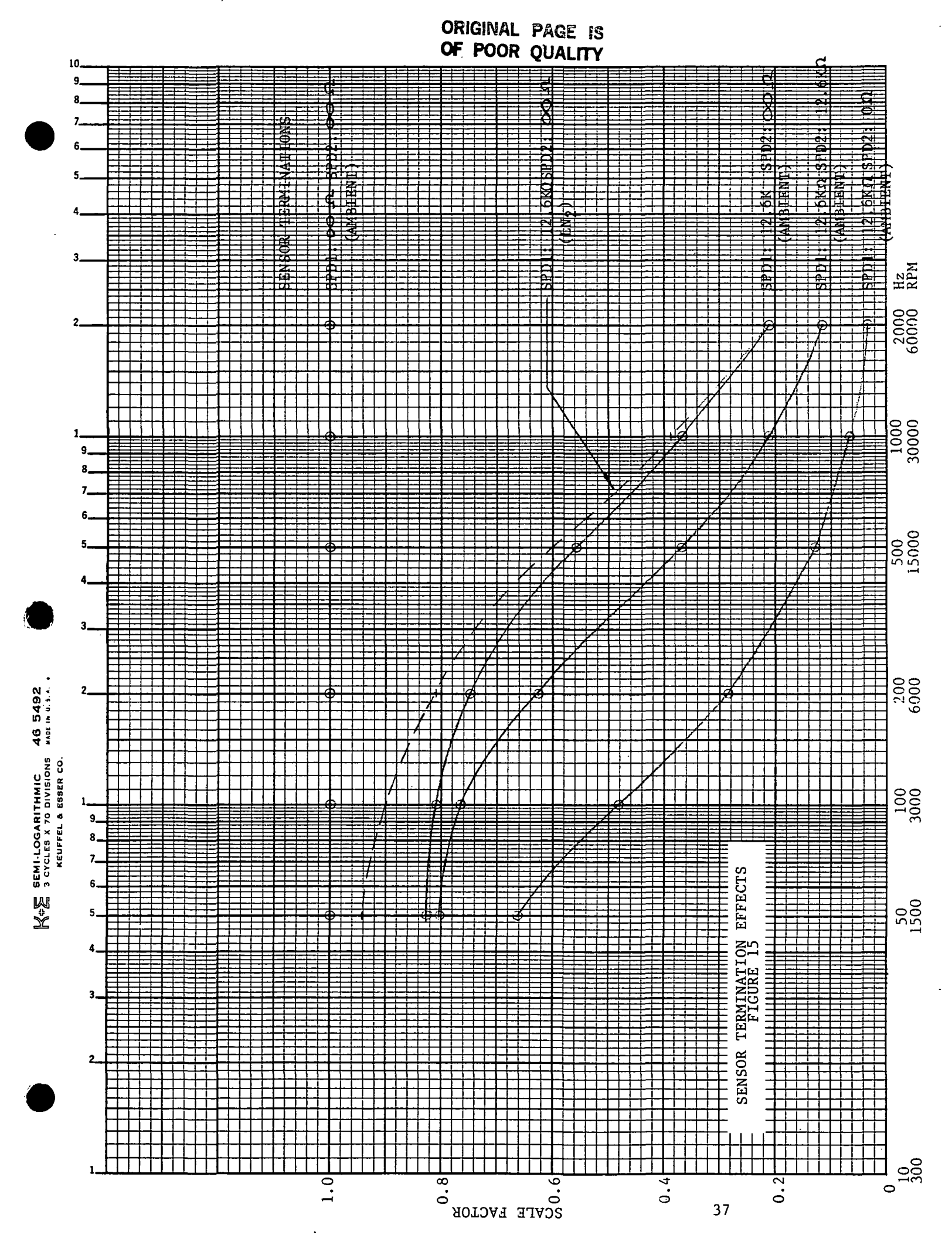

SENSOR TERMINATION EFFECTS
FIGURE 15

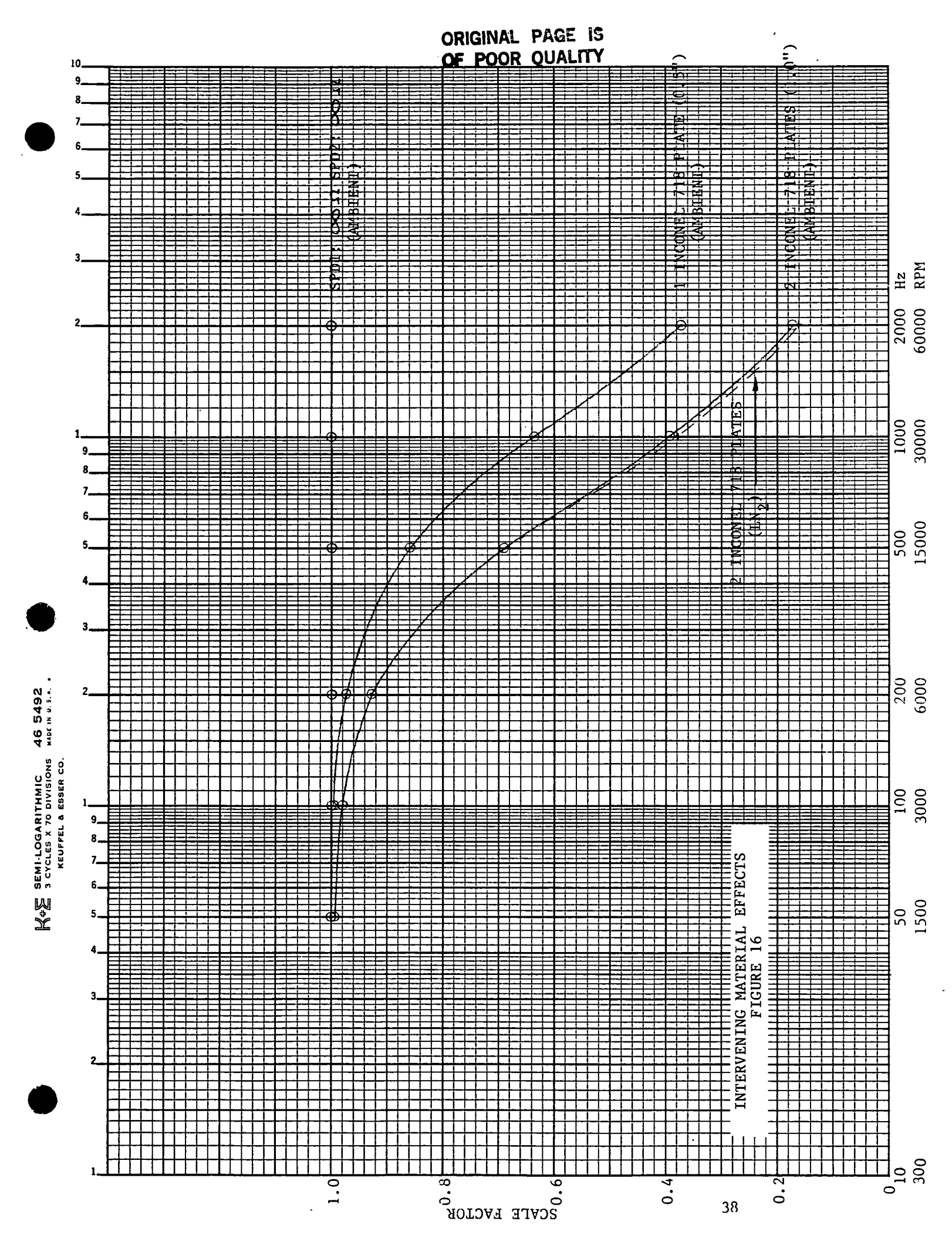

It is important to note that the existence of the HPOTP speed sensor access port along the sensor axis does theoretically allow a small signal increase, but the contribution is not measurable even at the highest frequencies tested.

Intervening Inconel 718 Temperature: As the temperature of the intervening material decreases, the resistivity of Inconel 718 decreases slightly. This effect allows eddy currents to be more readily induced in the material. This effect is very small (less than 4% signal loss), and only appears at the highest frequencies (Figure 16).

Magnet Temperature: One of the criteria leading to the selection of Crumax 35 for the speed nut magnet material was its magnetic field strength increase with decreasing temperature. This, however, was only found to be true to approximately -50°F to -100°F. The observed field strength from a Crumax 35 magnet at LN_2 temperature (-320.8°F) is 14.7 per cent less than that observed at ambient temperatures. This factor is constant for all frequencies.

Speed Sensor Characterization Summary

As presently designed, the non-intrusive speed-sensor provides sufficient output signal to meet the 1500 rpm requirement of 75mV. The signal level increases linearly with insignificant shielding, termination, and inductance effects at low rpm, and the sensor can be characterized by the number of turns on the coil, the coil area, and the core material and design. At higher rpm, the shielding, termination, and inductance effects dominate and bring the output signal level slightly below 75mV. Cryogenic temperature contributions are measurable, but generally small compared to the above effects.

NON-INTRUSIVE SPEED SENSOR IMPROVEMENTS

The breadboard non-intrusive speed sensor meets the 75mV peak output voltage requirement at 1500 rpm, but may require improvement at the higher rpm, depending upon the specific application. The most intuitive change to be considered involves increasing the number of turns on the sensor coils to boost the high rpm performance. Figure 17 shows the laboratory comparison between the 9150-turn and the 10000-turn sensors. While this approach very effectively increases the output voltage at low rpm, it is detrimental to sensor performance at high rpm. This is due to the increased coil inductance with increased turns, increased eddy current losses within the sensor core, and the very low terminating resistance (12.6 Kohms) observed by the sensor.

Although the intuitive approach does not provide the anticipated improvement, the reasoning as to why this approach fails does provide a very effective solution to the improvement issue. An experimental evaluation of solid cores (as presently exist in the speed sensor) and laminated cores inserted into an unhoused laboratory coil resulted in the data plotted in Figure 18. The laminated core, composed of many insulated layers of core material oriented parallel to the sensor axis, prevents large-scale eddy currents from flowing in the core. The system with the laminated core exceeds the solid core performance by 22% at 1500 rpm, 41% at 15000 rpm, and 30% at 40000 rpm.

ORIGINAL PAGE IS
OF POOR QUALITY

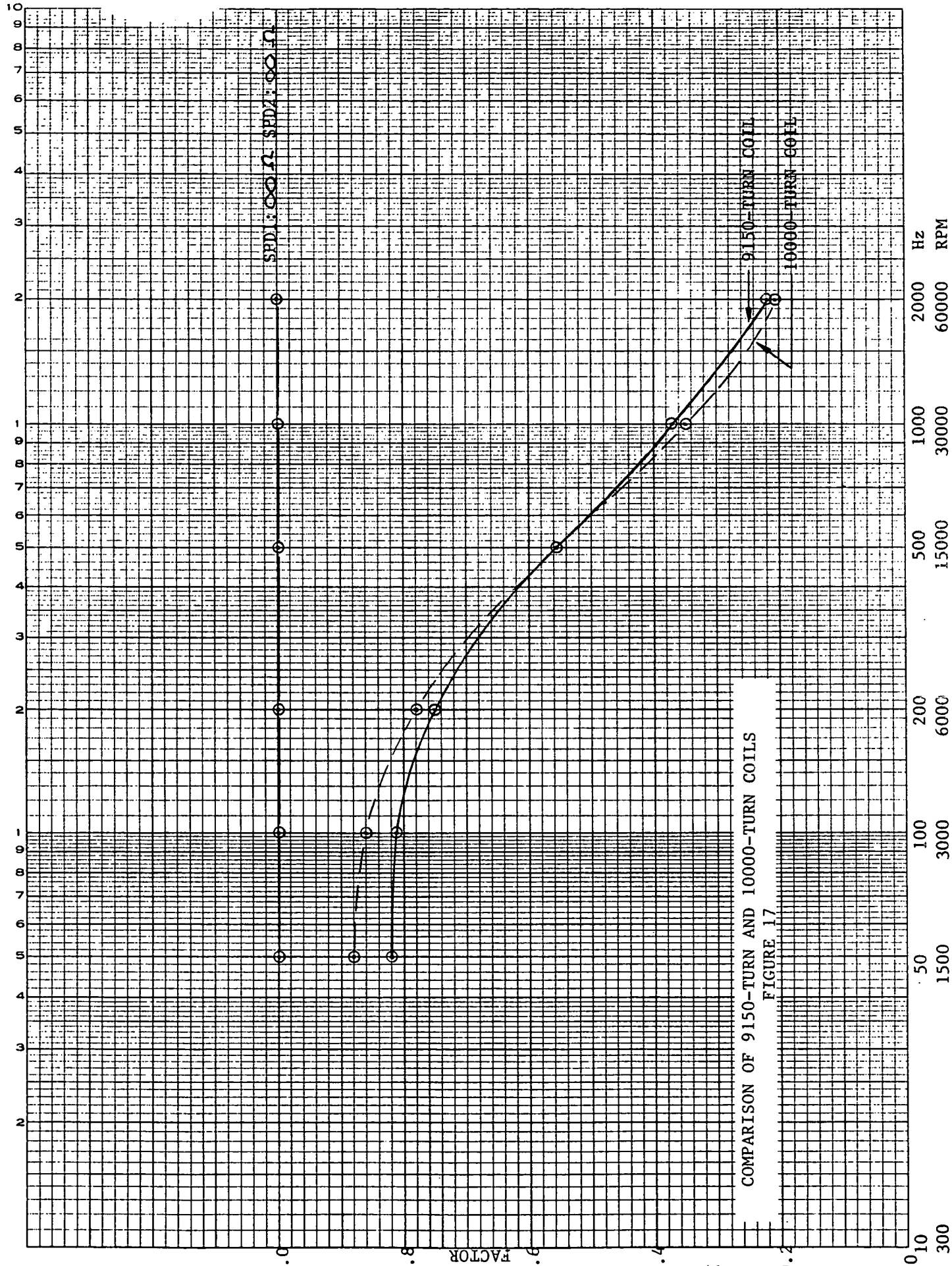

COMPARISON OF 9150-TURN AND 10000-TURN COILS
FIGURE 17

ORIGINAL PAGE IS
OF POOR QUALITY

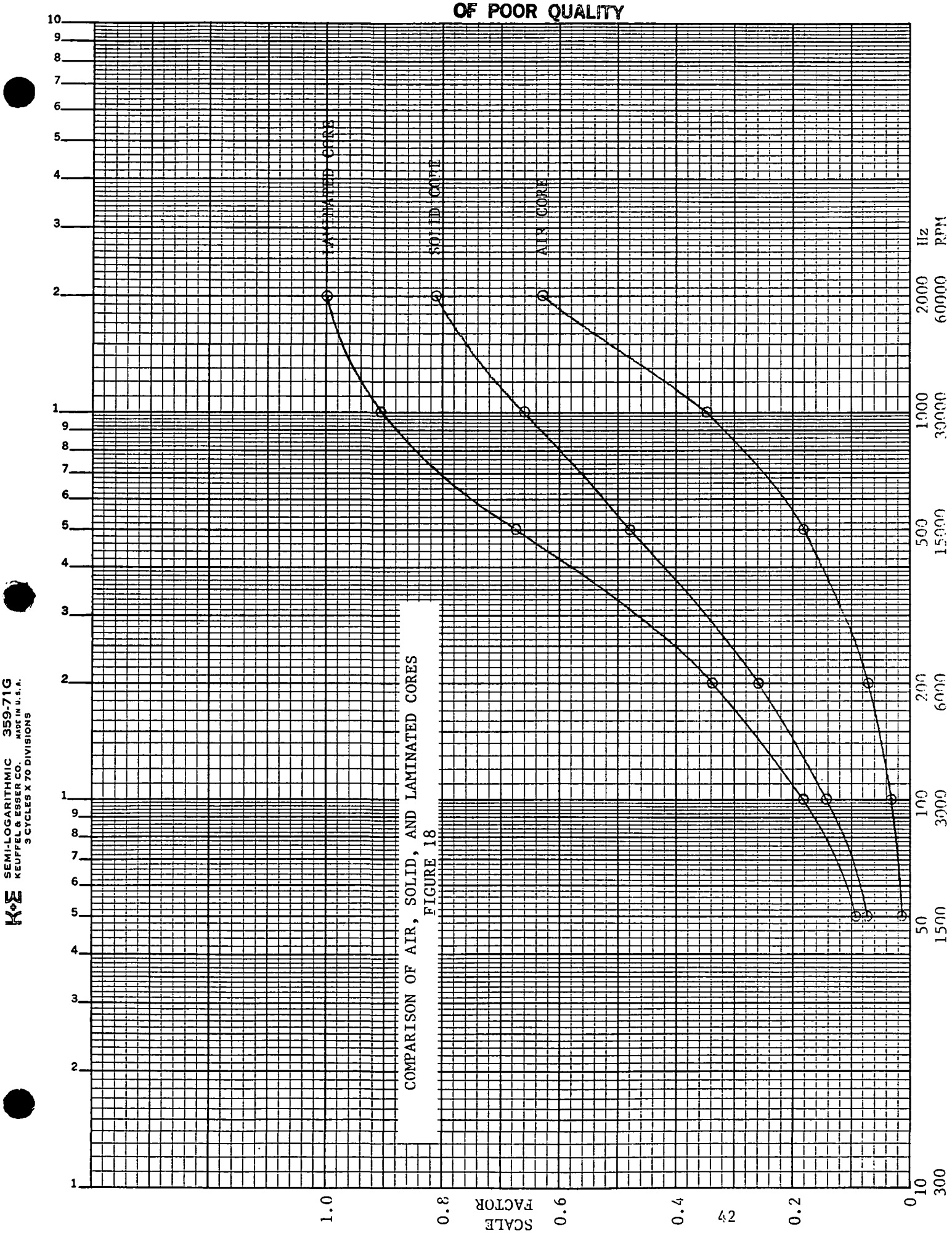

COMPARISON OF AIR, SOLID, AND LAMINATED CORES
FIGURE 18

The signal increases over the whole rpm range allow the reduction of the number of turns on the coils to further improve the high rpm performance (if required) while still meeting the 1500 rpm requirement. If the number of turns were reduced, the sensor coils could be made shorter, and, more effectively, windings could be removed from the inside of the coils. This approach would result in an increased average coil area which would further increase the output signal voltage while potentially reducing the sensor dimensions.

RECOMMENDATION

It is recommended that the breadboard non-intrusive speed sensor be refined and adapted for use on all SSME turbopumps to provide reliable shaft speed data for closed-loop control purposes.

ACKNOWLEDGEMENTS

We gratefully acknowledge the direction of T. Marshall, S. Morea, and R. Richards for their help in overseeing this program, which was funded by NASA's Marshall Space Flight Center under contract number NAS8-34658. We additionally recognize the support of Professor Charles Wilts of Caltech in the theoretical analysis and experimental verification of the non-intrusive speed sensor. We would also like to thank G. Roberts, A. Thurman, and E. Federoff and for their excellent technical support and mechanical design, F. Schuler and M. Browning for their electroplating expertise, and M. Burrus and R. Prock for coordinating the spin test effort at the Rocketdyne Engineering Development Laboratory.